JOURNAL OF SOLID STATE CHEMISTRY **96**, 162–168 (1992)

In Situ X-ray Studies on the Formation of Layered $Cs_x(H_2O)_y[NbS_2]$ via Staging Intermediates

W. PAULUS,* H. KATZKE,† AND R. SCHÖLLHORN†,[1]

**CEA-CNRS, CEN Saclay, Lab. Léon Brillouin, F-91191 Gif sur Yvette, France; and †Institut für Anorganische und Analytische Chemie, TU-Berlin, W-1000 Berlin 12, Germany*

Received August 22, 1991

Single crystal and powder electrodes of 2H–NbS_2 have been intercalated with hydrated Cs^+ ions forming $Cs_x(H_2O)_y[NbS_2]$. Structural investigations have been performed *in situ* during the intercalation reaction on single crystals which were aligned on a powder diffractometer in a specially equipped electrochemical cell. Several intermediate phases were obtained, showing a complex X-ray pattern with sharp, broad, and diffuse reflection profiles simultaneously, which also do not fit to integral *hkl* values. They can be interpreted, however, assuming a statistical disordered layer sequence of fully occupied and empty interlayer gaps. The structural disorder is confirmed by simulation calculations of the X-ray patterns.

Introduction

Intercalation compounds of transition metal dichalcogenides (MCh_2) with layered structure have been extensively studied during the last two decades (*1–3*). They represent a system of compounds with a tremendous variety of guest species as ions and molecules with different size, geometry, and composition. The quasi-two dimensional sandwich type layer sheets are coupled only by relatively weak van der Waals forces resulting in a strong anisotropic bonding behavior. Due to this almost poor interaction, they can be easily separated during intercalation. These materials are not only interesting because of their unusual physical properties, but also from a chemical point of view, as they may serve as fast electron/ion conductors and can also undergo selective ion exchange reactions rapidly (*4, 5*). Moreover, they are able to cointercalate suitable solvent molecules in addition to the guest cations forming polyelectrolytes with the capability to exchange both the cations and solvent molecules selectively in a reversible mode (*6*). Among these complex cointercalation systems only limited and mostly general information is available on the structure and the mechanism of their formation via solid state reactions (*7–11*). We have therefore decided to investigate the intercalation reaction of the monovalent alkali ions ($A^+ = Li^+, Na^+, K^+, Rb^+$, and Cs^+) into the hexagonal 2H–NbS_2 from aqueous electrolytes by *in situ* X-ray and neutron diffraction techniques. These phases are known so far as nonstoichiometric compounds with a large phase range. They can be prepared via topotactic redox reaction by chemical

---

[1] To whom correspondence should be addressed.

0022-4596/92 $3.00

electrolysis methods when switching NbS_2 battery electrodes as the cathode, or by chemical reduction. The reaction proceeds according to

$$xA^+ + xe^- + yH_2O + NbS_2 \leftrightarrow A_x^+(H_2O)_y[NbS_2]^{x-}. \quad (1)$$

Thereby each alkali cointercalation compound has its special peculiarities, mainly attributed to the size and solvation energy of the specific cation. For Li^+ and Na^+, two hydrate phases have been reported with an additional layer separation of 3 and 6 Å, respectively, which are related to the formation of a mono- or bilayer of H_2O molecules—H_2O has a van der Waals diameter of ≈2.8 Å—between the NbS_2 layer sheets (*4, 12, 13*). Investigations at different partial pressures of water, however, reveal a much more complex situation depending on the H_2O stoichiometry. According to the lower hydratation energy, only monolayer water hydrates were observed in case of the K^+, Rb^+, and Cs^+ ions. The maximum water content for the $A_x^+(H_2O)_y[NbS_2]^{x-}$ compounds is $y = \frac{2}{3}$ for $x = \frac{1}{3}$ in case of the H_2O monolayer systems, with a value of $x + y \leq 1$ and $y = 2$ for the bilayer systems. For the latter, one of the cations may be located in between the two H_2O layers, allowing the higher water stoichiometry.

In this paper we shall concentrate on our investigations of the formation of $Cs_x^+(H_2O)_y[NbS_2]^{x-}$ with a special focus on the reaction intermediates by X-ray diffraction techniques. Regarding the other hydrates with H_2O monolayer structure, the additional layer spacing (δd) is 3.23 Å for $Cs_{1/3}^+(H_2O)_y[NbS_2]^{1/3-}$, which is slightly but significantly higher than that reported for the corresponding compounds with $A^+ = K^+$, Rb^+, and NH_4^+ and $\delta d = 3.00 \pm 0.04$ Å, which can be related to the larger diameter of Cs^+ as compared to water (*4*).

Experimental

Stoichiometric 2H–NbS_2 was obtained by vapor phase transport at high temperatures from the elements. In order to avoid excess Nb atoms between the layers, leading to nonstoichiometric but well crystallizing $Nb_{1+x}S_2$, the reaction was performed under increased sulfur pressure. For this purpose a Nb/S mixture (Nb: Ventron, −325 mesh, 99.8%; S: Riedel de Häen, 99.98%) of about 10 g with a molar ratio of 1 : 2.5 was heated in sealed and evacuated quartz ampoules of 20 cm in length and 2 cm in diameter. NbS_2 crystals were transported in a two zone furnace from 970°C → 940°C with iodine (5 mg/cm^3) used as carrier. The crystals grew over a period of 20 days and were quenched in an ice/water mixture. 2H–NbS_2 polycrystalline material was obtained after 10 days isothermal annealing at 950°C. The crystals consist of metallic black platelets up to (10 × 10 × 1) mm in size, showing an uneven surface. Lattice parameters were determined from powder X-ray investigations to be $a = 3.319(2)$ and $c = 11.955(6)$ Å. The stoichiometry was determined, by oxidizing NbS_2 to Nb_2O_5 at 900°C in air, to be $Nb_{0.999(2)}S_2$, which is close to the ideal value. The cathodic reduction of pressed powder and crystal 2H–NbS_2 electrodes was performed at ambient temperature in aqueous 1 *N*-alkalisulfate electrolyte. Platinum counter and Ag/AgCl reference electrodes, the latter very closely connected to the battery electrode, were used. *In situ* X-ray diffraction studies have been carried out in a specially equipped electrochemical cell which was aligned on a powder diffractometer (Siemens D500, Cu anode, 8–28 mode) with primary monochromator and a fast position sensitive detector (Braun). The cell was made out of plexiglass; the reaction chamber was covered by a thin X-ray amorphous adhesive tape. One side of the crystal was stuck to the tape, while a thin platinum wire was affixed with carbon paste to the backside of the crystal. A more detailed description of the X-ray geometry and electrochemical cells is given elsewhere (*14*). The applied current density did not exceed 100 μA/cm^2 with respect to the active reaction surface, i.e., the front side in the case of the crystals. The diffractograms were recorded every 30 min with the crystal under constant current (Knick galvanostat, J 150), yielding a resolution in stoichiometry of better than $x = 0.01$.

Results and Discussion

The crystalline quality of 2H–NbS_2 strongly depends on its stoichiometry. Highly ordered material with a low rate of stacking faults is only available when excess Nb atoms enter the empty octahedral sites between the layers. We shall discuss the relation of the crystalline quality to stoichiometry and reactivity in more detail elsewhere (*14*). Since the as prepared 2H–$Nb_{0.999(2)}S_2$ is quasi stoichiometric, the crystalline quality is expected to be poor, which can in fact be deduced from sharp 00*l* and *hk*0 reflections, whereas all mixed *hkl* reflections show a remarkable profile broadening. This has to be attributed to a one dimensional stacking disorder of the NbS_2 layer sheets, implying a good requirement to expect a high reactivity for intercalation reactions. Although we know the used 2H–NbS_2 material is highly disordered, we shall use the term single crystal for the grown NbS_2 platelets.

Electrochemical Investigations

The potential/charge transfer curve of the galvanostatic reduction of a 2H–NbS_2 single crystal is given in Fig. 1. From relaxation studies, the measured potential of the used single crystal battery electrode was confirmed to be close to the equilibrium state. The value of the charge transfer n (mole electrons/mole NbS_2) is restricted to $n \approx 0.5$ while the potential of the hydrogen discharge H_3O^+/H_2 is reached. From the simple rigid band model, an electron transfer of n up to 1 should be possible (*15*). In the range $0 \leq n \leq 0.27$, 4 two phase regions can be derived from the almost flat potential steps. Corresponding to the first step between $0 \leq n \leq 0.09$, the reflection intensity of the NbS_2 host lattice decreases rapidly, while new reflections of the first intermediate phase occur. Up to $n \approx 0.14$ the growth of the second intermediate phase occurs; subsequently, a very small plateau of $\delta n \approx 0.01$ follows, which can only be resolved with single crystals and not with polycrystalline powder electrodes. During the fourth plateau between $0.15 \leq n \leq 0.27$ a $Cs^{+}_{0.27}(H_2O)_y[NbS_2]^{0.27-}$ phase comes up, which can be indexed hexagonal with $a = 3.352(5)$ and $c = 18.51(2)$ Å, representing a H_2O monolayer phase with completely filled interlayer gaps. The differences in the potentials of these four phases are very small, indicating that the change in lattice energy during intercalation is relatively small.

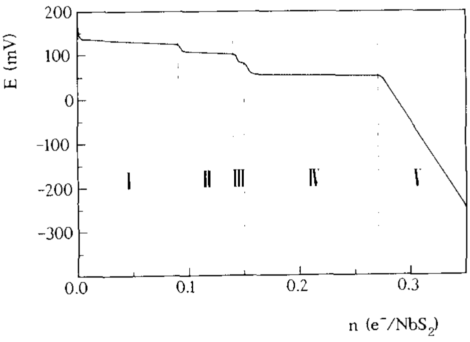

FIG. 1. Potential/charge transfer curve for the galvanostatic reduction of a 2H–NbS_2 single crystal electrode in aqueous 1*N*-Cs_2SO_4 electrolyte (*E* vs Ag/AgCl).

The determined values of n given above differ slightly from crystal to crystal and are especially reduced when pressed powder electrodes are used. A variance of δn up to a value of 0.05 was observed. The estimated lower electron transfer in the case of powder electrodes gives rise to the assumption that parallel to the galvanostatic controlled intercalation reaction a partial hydrolysis of the NbS_2 lattice takes place. Such parasitic redox reactions are known for similar reaction systems of layered dichalcogenides in aqueous electrolytes, resulting in the formation of polysulfide anions or elemental sulfur (*5*):

$$2xOH^- + MS_2 \rightarrow MS_{2-x}O_x + xS^{2-} + xH_2O$$

$$xS^{2-} \rightarrow x/8S_8 + 2xe^-$$

$$xe^- + MS_{2-x}O_x \rightarrow [MS_{2-x}O_x]^{x-}.$$

The synchronously generated electrons are then able to reduce the host lattice while an equivalent amount of hydrated cations is "autointercalated." For powder electrodes, the hydrolysis sensitive crystallite surface is more pronounced as compared to single crystal electrodes. In that sense the charge transfer shifts to lower rates can be understood qualitatively. The values of n obtained from galvanostatic reduction experiments may therefore be regarded as minimum values, the real values being up to $\delta n \approx 0.05$ higher.

Structural Investigations

Structural changes during the intercalation reaction were studied under applied potential using crystals of about (3 × 3 × 0.1) mm in size *in situ*. The fairly low thickness guarantees that although X-rays were used, the structural information obtained represents the major part of the whole crystal. Due to the alignment of the crystals described above, only the 00l reflection series can be observed. A selective collection of the obtained X-ray patterns is shown in Fig. 2; the change of the peak positions and intensity with n is given in Fig. 3(a) and (b).

During the formation of the first intermediate phase between $0 \leq n \leq 0.09$, a continuous decrease of the 2H–NbS_2 reflections to the value of the background level is observed, while new reflections of the first intermediate start to increase. Around every 00l reflection of NbS_2, with $l = 4n + 2$, broad and intense pairs of "satellite" reflections are developed which can no longer be indexed with integral *hkl* indices. In addition, they show two surprising and unusual features. The first is related to the positions of these reflections which vary to higher and to lower scattering angles. With respect to the orientation of the crystal, they are all expected to belong to changes in the c-axis of the intercalation compound and therefore should shift either to higher *or* to lower scattering angles, correlated to a decrease *or* increase of the c-axis. The second is the unusual distribution of the full width half maxima (FWHM) for one single pattern. Besides sharp peaks, there also exist some with a broad, and in few cases nearly diffuse, profile. This second fact signifies that one cannot interpret the latter behavior as a particle size effect of different domains. For the second two phase region the peak positions remain nearly constant, but here also sharp and broad profiles exist simultaneously, which also do not fit to integral *hkl* indices. The third small plateau between $0.14 \leq n \leq 0.15$ cannot be resolved structurally, either by changes in the peak position or by variations in the FWHM. During the last plateau up to $n \approx 0.27$ almost sharp reflections occur with values in the FWHM of 0.1° in 2θ, which is comparable to the unreacted 2H–NbS_2 host lattice. Contrary to the latter, where all mixed *hkl* values were found to be broad due to the stacking disorder, the reflections for $Cs^+_{0.27}(H_2O)_y[NbS_2]^{0.27-}$ show narrow profiles, as can be determined from Debye–Scherrer exposures with the compound under liquid electrolyte. This implies a larger less pronounced disorder for the intercalation compound, which may be explained by the coupling mechanism of the layer sheets. For the intercalated lattice, forces with ionic–dipolar character (Cs^+–$S^{\delta-}$ and $H^{\delta+}$–$S^{\delta-}$) are able to induce a lattice rearrangement. This behavior is quite unusual, hence the lattice disorder normally increases during intercalation, which is mainly attributed to an inhomogenious distribution of the intercalant species.

During the formation of the first interme-

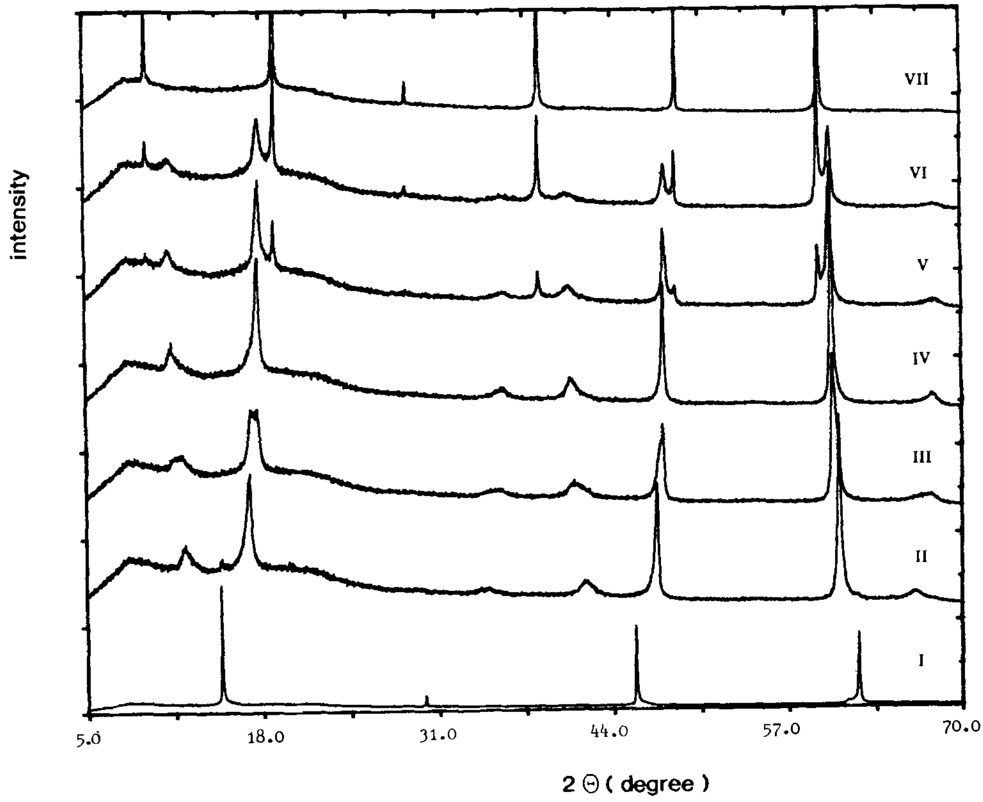

FIG. 2. X-ray patterns, obtained *in situ* during the intercalation of hydrated Cs^+ ions into 2H–NbS_2 single crystals for different *n*: (I), 2H–NbS_2; (II), $Cs_{0.09}(H_2O)_yNbS_2$; (IV), $Cs_{0.14}(H_2O)_yNbS_2$; (VII), $Cs_{0.27}(H_2O)_yNbS_2$; (III), (V), and (VI) show intermediate steps.

diate, one can estimate reflection broadenings up to 1.1°, for the second intermediate up to 0.6° for the FWHM in 2θ. Figure 3a shows the change of the normalized intensity of selected peaks for each phase versus *n*. Comparison to the potential/charge transfer curve reveals that the maxima directly correspond to the specific potential steps, as one would expect for subsequent two phase regions. This does not, however, hold for the small region at $n \approx 0.15$ without any anomality in the intensity variation. Beyond the fourth two phase region the intensity decreases continuously with *n*, in agreement with the assumed one phase region. This is also reflected by the continuous decrease in the *c*-axis parameter from $c = 18.51$ Å at $n \approx 0.27$ to 18.25 Å at $n \approx 0.5$, as determined from the 002 reflection during the intercalation reaction without any significant changes in the FWHM.

Structural investigations reveal that one can understand the behavior in the peak shift and broadening when assuming a statistical disorder in the layer sequence of the empty host lattice with a *c*-axis of 11.96 Å and the fully intercalated phase with a *c*-axis of 18.51 Å. Calculations of this model were carried out on the basis of the Hendrix–Teller formalism (*16*), which were directly computed after the more general expression given in (*17, 18*). The calculated

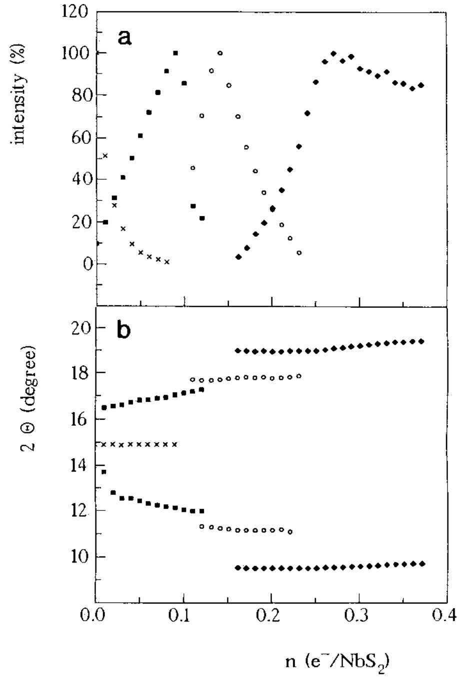

FIG. 3. Changes in the intensity (a) and position (b) of selected reflections during the intercalation of hydrated Cs^+ ions into 2H–NbS_2 single crystals vs n.

diffractograms are given in Fig. 4 for a scattering angle between 8° and 21° for Cu$K_{\alpha 1}$ wavelength. They are not corrected for intensity, because the structure of the fully intercalated phase is not yet known. Instead, an equal structure factor for both phases was taken into account. The patterns were calculated for statistical mixtures with a volume fraction between 10 and 90%. Above and below these values, the FWHM is no longer predominantly determined by the stacking faults of the compound but becomes more dependent on the diffractometer geometry, a fact which has not been taken care of in these simulations.

In this model one can rule out the ratio of occupied and unoccupied layers directly by comparison between the measured and calculated peak positions. The first reflections visible for the first intermediate phase can thus be related to a compound with a ratio of unoccupied to occupied interlayer gaps of around 2 : 1, i.e., on the average and statistical scale one-third of all layers are intercalated. This ratio shifts to 3 : 2 when n increases to 0.09. For the second intermediate phase, a nearly constant ratio is found to be around 1 : 1 which formally corresponds to a second stage phase, here realized to be distributed statistically. On the basis of the estimated ratios, one can predict the maximum stoichiometry with respect to the water, which is $Cs_{0.09}^{+}(H_2O)_{0.31}[NbS_2]^{0.09-}$ for the first and $Cs_{0.14}^{+}(H_2O)_{0.36}[NbS_2]^{0.14-}$ for the second intermediate phase.

Although the measured X-ray patterns can be explained assuming a statistical distribution of filled and empty layers, there are still some contradictions from a thermodynamical point of view, with the idea arising from the flat potential step that a two phase region has to be assumed for the first intermediate phase. Regarding the continu-

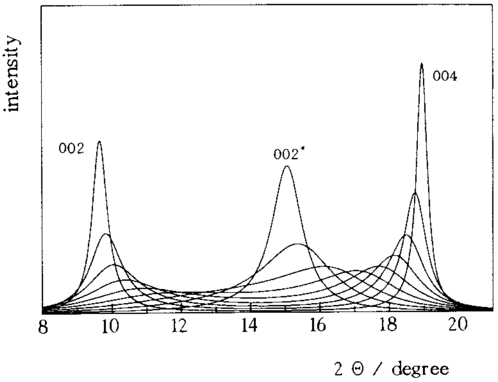

FIG. 4. Simulated diffractograms of a phase with a statistical disorder of the layer sequence with c = 11.96 Å and c = 18.51 Å for different volume fractions. The patterns were calculated between ratios of 10/90 and 90/10 for the two distances. The splitting of the 002 reflection of 2H–NbS_2 (asterisk) turns continuously to the 002 and 004 reflection of the new intercalation compound $Cs_{0.27}(H_2O)_yNbS_2$. Note that the marked reflections are already mixtures of 10/90 or 90/10 ratios of the different layer separation.

ous peak shifts in this region, one would suggest that a one phase rather than a two phase system is present here. This unusual behavior may also be explained with the statistical distribution of empty and occupied layers and their relation to micro- and macroscopic symmetry.

If we assume a host lattice suitable for intercalation reactions, the reaction normally takes place via an ordered framework lattice; i.e., all the intermediate phases usually show a long range order. For the as observed intermediates this is definitely not the case. Here we only observe a change in the ratio of occupied and unoccupied layers, but on a microscopic scale we may regard the empty lattice as part of the unreacted NbS_2 host lattice, while the filled layers represent the new intercalation compound. Because of the averaging, resulting from the X-ray coherence length of around 500 Å, we are only able to see the mean value of all distributions, here the amounts of specific layers on a somewhat macroscopic scale. The chemical potential is in a first approximation not strongly affected by the size of empty and occupied layer packages, respectively, and especially not for metallic conductors, because of the averaging of the different Fermi levels. The result should therefore be the same for statistically mixed or ordered lattices. In that way the shifts in the peak position for the first intermediate are not necessarily an unambiguous indicator for a one phase region and are therefore not in contradiction to the observed flat potential step.

The reaction described can be reversed when switching $Cs_{0.27}^{+}(H_2O)_y[NbS_2]^{0.27-}$ as the anode in the electrochemical cell described above. After a charge transfer of $n = 0.27$, the NbS_2 lattice is retained, showing reflection profiles broader than the unreacted starting material. This confirms the assumption of a partial hydrolysis of the host lattice during intercalation. The change in the peak positions and intensity of the intermediate phases were found to run reverse to the intercalation reaction; the same is valid for their line broadenings.

Acknowledgment

This work has been supported by the Bundesminister für Forschung und Technologie.

References

1. G. V. SUBBA RAO AND M. W. SHAFER, *in* Intercalated Layered Materials" (F. Lévy, Ed.), p. 99, Reidel Publ., Dordrecht, Holland (1979).
2. J. ROUXEL, *in* "Intercalated Layered Materials" (F. Lévy, Ed.), p. 201, Reidel Publ., Dordrecht, Holland (1979).
3. R. SCHÖLLHORN, *in* "Intercalation Chemistry" (S. Whittingham, Ed.), p. 315, Academic Press, New York (1982).
4. A. LERF AND R. SCHÖLLHORN, *Inorg. Chem.* **16,** 2950 (1977).
5. R. SCHÖLLHORN, E. SICK, AND A. LERF, *Mater. Res. Bull.* **10,** 1005 (1975).
6. R. SCHÖLLHORN AND H. MEYER, *Mater. Res. Bull.* **9,** 1237 (1974).
7. A. J. A. BOS-ALBERINK, R. J. HAANGE, AND G. A. WIEGERS, *J. Less-Common Met.* **63,** 69 (1979).
8. C. RIEKEL, H. G. REZNIK, AND R. SCHÖLLHORN, *J. Solid State Chem.* **34,** 253 (1980).
9. E. SANDRÉ, R. BREC, AND J. ROUXEL, *J. Solid State Chem.* **88,** 269 (1990).
10. M. RIPERT, J. PANNETIER, Y. CHABRE, AND C. POINSIGNON, *in* "MRS Fall Meeting, Boston (1990)," preprint.
11. H. A. GRAF, A. LERF, AND R. SCHÖLLHORN, *J. Less-Common Met.* **55,** 213 (1977).
12. D. C. JOHNSTON, *Mater. Res. Bull.* **17,** 13 (1982).
13. D. C. JOHNSTON, *J. Less-Common Met.* **84,** 327 (1982).
14. W. PAULUS, H. KATZKE, AND R. SCHÖLLHORN, in preparation.
15. J. A. WILSON AND A. D. JOFFE, *Adv. Phys.* **18,** 193 (1969).
16. S. HENDRIX AND E. TELLER, *J. Chem. Phys.* **10,** 147 (1942).
17. D. HOHLWEIN AND W. METZ, *Z. Kristallogr.* **139,** 279 (1974).
18. D. HOHLWEIN, Thesis, University of Hamburg (1972).